THE CATHOLIC UNIVERSITY OF AMERICA
DEPARTMENT OF ELECTRICAL ENGINEERING

JOINT-SPACE ADAPTIVE CONTROL OF A 6 DOF END-EFFECTOR WITH CLOSED-KINEMATIC CHAIN MECHANISM

Charles C. Nguyen
Principal Investigator and Associate Professor
and
Zhen-Lei Zhou
Graduate Research Assistant

submitted to
Mr. David E. Provost
Code 735.1
Goddard Space Flight Center (NASA)
Greenbelt, Maryland

August 1989

SUMMARY

This semi-annual report presents the research results from the research grant entitled "Active Control of Robot Manipulators," funded by the Goddard Space Flight Center, under the Grant Number NAG 5-780, for the period between February 1, 1989 and August 1, 1989.

In this report, we present the development of a joint-space adaptive scheme that controls the joint position of a six-degree-of-freedom (DOF) robot end-effector performing fine and precise motion within a a very limited workspace. The end-effector was built at NASA to study autonomous assembly of NASA hardwares in space. The design of the adaptive controller is based on the concept of model reference adaptive control (MRAC) and Lyapunov direct method. In the development, we assume that the end-effector performs slowly varying motion. Computer simulation is performed to investigate the performance of the developed control scheme on position control of the end-effector. Simulation results manifest that the adaptive control scheme provides excellent tracking of several test paths.

1 INTRODUCTION

Recognizing the fact that performing operations in space is dangerous, NASA has paid its attention to the research of *telerobotics* which is the combination of two different concepts, *teleoperation* and *robotics* [1]. Telerobotic operations can be executed either in a *traded control* mode (serial operation) or in a *shared control* mode (parallel operation). In the traded control mode, using teleoperation the human operator performs some portion of a task and then let the telerobot perform some other portion of the task autonomously while on the other hand, the human operator and the telerobot perform portions of the task simultaneously in a shared control mode. In either modes, successful robotic tasks require that the motion of the telerobot be controlled precisely. A telerobotic system generally consists of a *master arm* and a *slave arm*. It has been proposed [2] that a light and compact 6 DOF end-effector be built and mounted to the slave arm to autonomously perform fine and precise motion during the traded mode of the telerobotic operation. In this report we present the development of a joint-space adaptive control scheme for controlling the end-effector motion by using the concept of MRAC and Lyapunov theorem.

When a dynamic model can accurately represent the real end-effector dynamics, then *computed torque* [3] scheme whose development is mainly based on the dynamic model, can be employed to control the end-effector motion. Using the above scheme, time-varying controllers can be designed so that disturbances are minimized and excellent tracking performance can be achieved. Since it is relatively difficult, if not possible to derive an accurate dynamic model for a robot end-effector, the computed torque scheme is not feasible. The urgent need of a control scheme that is able to effectively react to the presence of nonlinearities and uncertainties in robot end-effector dynamic model and payloads has motivated the research of adaptive control schemes, according to a recent survey [4]. MRAC method and Lyapunov theorem function were employed by several researchers to design adaptive controllers for cartesian- and joint-space trajectory control, which was proved to provide global stability [5,6]. Lim and Eslami [7] considered the design of robust adaptive controllers. Adaptive force control problem was investigated by Daneshmend and Pak [8] for a cutting problem. In [9] Houshangi and Koivo designed an adaptive force-position controller with self-tuning in cartesian space by using eigenvalue assignment method and minimization of a quadratic performance criterion. Recently, Seraji [10] presented the implementation of adaptive force and position controllers for robot manipulators within the hybrid control structure using an improved MRAC. The problem of hybrid control of force and position was also considered by Nguyen and Pooran [11].

In this report, we first describe the structure of a 6 DOF end-effector built at NASA to study telerobotic assembly. We then present the derivation of a joint-space adaptive control for controlling the end-effector motion. After that, the developed control scheme will be applied to control the planar motion of a 2 DOF end-effector built in our robotic laboratory. Discussion of the simulation results and recommendation for future research direction will conclude the report.

Notations used in this report are listed below

- $\mathbf{M}^T$: transpose of the matrix $\mathbf{M}$
- $\mathbf{0}_n$: (nxn) matrix whose elements are all zero
- $\mathbf{I}_n$: (nxn) identity matrix

2 THE CKCM ROBOT END-EFFECTOR

Most telerobotic assembly of parts such mating or fastening can be accomplished in a *traded control mode*[1] in which using the master arm, the human operator remotely moves the slave arm into the assembly workspace and then let a robot end-effector, mounted to the end of the slave arm perform the assembly task autonomously. In addition to the requirements of compactness and lightweight, the end-effector must be able to perform very precise motion within a very limited workspace. In order to study the feasibility of autonomous assembly of parts in a telerobotic operation, an end-effector whose size is about ten times that of the telerobot end-effector was designed and built at the Goddard Space Flight Center (**GSFC**) [12] and is currently located at the Center for Artificial Intelligence and Robotics (**CAIR**)[1]. As shown in Figure 1, the end-effector resembles the structure of the Stewart platform [13], and mainly consists of an upper payload platform, a lower base platform and six linear actuators. The movable payload platform is supported above the stationary base platform by six axially entensible rods where in order to provide the extensibility, the system uses recirculating ballscrews that are driven by stepper motors. The motion of the payload platform is produced by the combination of extending and shortening the actuator lenghts. Each end of the actuator links is mounted to the platforms by 2 rotary joints with intersecting and perpendicular axes. The end-effector has 24 rotary joints, 6 prismatic joints, and 14 links including the 2 platforms and therefore has 6 DOF, which can be proved by applying the *number synthesis*[2].

3 THE JOINT-SPACE ADAPTIVE CONTROLLER

The robot end-effector described in previous section assumes a closed-kinematic chain mechanism (**CKCM**) which has been showed to possess high precision positioning capability [2]. Since CKCM end-effectors generally have a closed-form solution for its inverse kinematic problem, joint-space trajectory control scheme is proposed to control the end-effector motion so that time-consuming iterative computation of the forward kinematics in a Cartesian-space control scheme of CKCM end-effectors can be avoided. In other words, the error actuating signal to the joint actuators is computed based on the error between the desired variable and the actual variable. In addition, adaptive controllers are utilized instead of fixed-gain controllers in order to compensate the presence of nonlinearities and uncertainties in end-effector dynamics and payloads. Figure 2 presents the joint-space adaptive control scheme proposed to control the end-effector motion. As the figure shows, position sensors mounted on the end-effector actuators provide feedback information of the actual lenghts of the six actuators. The actual lenghts are then compared to the desired lenghts that are computed by the inverse kinematics from the desired Cartesian variables specified by the user or some path planner. The lenght difference will then serve as inputs to the adaptive controllers which in turn produce required joint forces for the actuators to track the end-effector along a desired trajectory.

If we denote a (6x1) vector l composed of six actuator lenghts l_i for i=1,2,...,6 such that

$$\mathbf{l} = (l_1\ l_2\ \ldots l_6)^T \tag{1}$$

[1]To test control schemes developed under a research grant with NASA/GSFC

as the joint variable vector, then the end-effector dynamics can be written as [11]:

$$\tau(t) = \mathbf{M}(\mathbf{l},\dot{\mathbf{l}})\,\ddot{\mathbf{l}}(t) + \mathbf{N}(\mathbf{l},\dot{\mathbf{l}})\,\dot{\mathbf{l}}(t) + \mathbf{G}(\mathbf{l},\dot{\mathbf{l}})\,\mathbf{l}(t) \tag{2}$$

where τ(t) denotes the (6x1) joint force vector, $\mathbf{M}(\mathbf{l},\dot{\mathbf{l}})$, the manipulator mass matrix is a symmetric positive-definite matrix of order (6x6), $\mathbf{N}(\mathbf{l},\dot{\mathbf{l}})$ and $\mathbf{G}(\mathbf{l},\dot{\mathbf{l}})$ are (6x6) matrices whose elements are highly complex nonlinear functions of $\mathbf{l}$ and $\dot{\mathbf{l}}$. In the right-hand side of (2), if we neglect joint friction, the second term represents the centrifugal and Coriolis forces, and the third term the gravity forces.

Consider now a PD time-varying controller defined by

$$\tau(t) = \mathbf{K}_p(t)\,\mathbf{l}_e(t) + \mathbf{K}_d(t)\,\dot{\mathbf{l}}_e(t) \tag{3}$$

where

$$\mathbf{l}_e(t) = \mathbf{l}_d(t) - \mathbf{l}(t) \tag{4}$$

represents the deviation of the actual joint vector $\mathbf{l}(t)$ from the desired lenght vector $\mathbf{l}_d(t)$. Furthermore, $\mathbf{K}_p(t)$ and $\mathbf{K}_d(t)$ denote the proportional and derivative adaptive controller gain matrices, respectively.

Substituting (3) into (2) we obtain

$$\mathbf{M}\,\ddot{\mathbf{l}}_e + (\mathbf{N}+\mathbf{K}_d)\,\dot{\mathbf{l}}_e + (\mathbf{G}+\mathbf{K}_p)\,\mathbf{l}_e = \mathbf{M}\,\ddot{\mathbf{l}}_d + \mathbf{N}\,\dot{\mathbf{l}}_d + \mathbf{G}\,\mathbf{l}_d \tag{5}$$

where the dependent variables of the matrices and vectors have been dropped for simplicity.

Defining a (12x1) state vector $\mathbf{z}(t)$ such that

$$\mathbf{z}(t) = \left[\mathbf{l}_e^T(t) \quad \dot{\mathbf{l}}_e^T(t)\right]^T \tag{6}$$

converts (5) into the state space representation described by

$$\dot{\mathbf{z}}(t) = \begin{bmatrix} \mathbf{0}_6 & \mathbf{0}_6 \\ -\mathbf{A}_1 & -\mathbf{A}_2 \end{bmatrix} \mathbf{z}(t) + \begin{bmatrix} \mathbf{0}_6 & \mathbf{0}_6 & \mathbf{0}_6 \\ \mathbf{A}_3 & \mathbf{A}_4 & \mathbf{I}_6 \end{bmatrix} \mathbf{u}(t) \tag{7}$$

where

$$\mathbf{A}_1 = \mathbf{M}^{-1}(\mathbf{G}+\mathbf{K}_p), \quad \mathbf{A}_2 = \mathbf{M}^{-1}(\mathbf{N}+\mathbf{K}_d), \tag{8}$$

and

$$\mathbf{A}_3 = \mathbf{M}^{-1}\,\mathbf{G}, \quad \mathbf{A}_4 = \mathbf{M}^{-1}\,\mathbf{N}, \tag{9}$$

and

$$\mathbf{u}(t) = \left[\mathbf{l}_d^T(t) \quad \dot{\mathbf{l}}_d^T(t) \quad \ddot{\mathbf{l}}_d^T(t)\right]^T. \tag{10}$$

In the framework of the model reference adaptive control (**MRAC**), the *adjustable system* is represented by Equation (7). The *reference model* specifies the desired performance of the end-effector in terms of $\mathbf{l}_e(t) = [l_{e1}(t)\; l_{e2}(t) \ldots l_{e6}(t)]^T$, which is the tracking error vector. Suppose the tracking errors $l_{ei}(t)$ for i=1,2,...,6, are decoupled from each other, and satisfy the relationship

$$\ddot{l}_{ei}(t) + 2\,\xi_i\,\omega_i\,\dot{l}_{ei}(t) + \omega_i^2\,l_{ei}(t) = 0 \tag{11}$$

for i=1,2,...,6, where ξ_i and ω_i denote the damping ratio and the natural frequency of l_{ei}, respectively. Then the reference model can be described by

$$\dot{\mathbf{z}}_m(t) = \mathbf{D}\,\mathbf{z}_m(t) = \begin{bmatrix} \mathbf{0}_6 & \mathbf{I}_6 \\ -\mathbf{D}_1 & -\mathbf{D}_2 \end{bmatrix} \mathbf{z}_m(t), \tag{12}$$

where $\mathbf{D}_1$=diag(ω_i^2) and $\mathbf{D}_2$=diag($2\xi_i\omega_i$) are constant (6x6) diagonal matrices, and

$$\mathbf{z}_m(t) = \left[\mathbf{l}_m^T(t) \quad \dot{\mathbf{l}}_m^T(t)\right]^T \tag{13}$$

with

$$\mathbf{l}_m = (l_{e1}\ l_{e2}\ \ldots l_{e6})^T. \tag{14}$$

The solution to (12) can be found as

$$\mathbf{z}_m(t) = \exp(\mathbf{D}t)\,\mathbf{z}_m(0) \tag{15}$$

which under the assumption that the initial values of the actual and reference lenghts are the same, i.e., $\mathbf{z}_m(0) = 0$, yields $\mathbf{z}_m(t) = 0$.

Now if the adaptation error vector e(t) is defined as

$$\mathbf{e}(t) = \mathbf{z}_m(t) - \mathbf{z}(t), \tag{16}$$

then from (7) and (12), we obtain an error system defined as

$$\begin{aligned} \dot{\mathbf{e}}(t) \;=\; & \begin{bmatrix} \mathbf{0}_6 & \mathbf{I}_6 \\ -\mathbf{D}_1 & -\mathbf{D}_2 \end{bmatrix} \mathbf{e}(t) + \begin{bmatrix} \mathbf{0}_6 & \mathbf{0}_6 \\ \mathbf{A}_1 - \mathbf{D}_1 & \mathbf{A}_2 - \mathbf{D}_2 \end{bmatrix} \mathbf{z}(t) \\ & + \begin{bmatrix} \mathbf{0}_6 & \mathbf{0}_6 & \mathbf{0}_6 \\ -\mathbf{A}_3 & -\mathbf{A}_4 & -\mathbf{I}_6 \end{bmatrix} \mathbf{u}(t). \end{aligned} \tag{17}$$

We proceed to select a Lyapunov function candidate $v(t)$ such that

$$\begin{aligned} v(t) \;=\; & \mathbf{e}^T\mathbf{P}\mathbf{e} + tr\left[(\mathbf{A}_1 - \mathbf{D}_1)^T\boldsymbol{\Pi}_1(\mathbf{A}_1 - \mathbf{D}_1)\right] \\ & + tr\left[(\mathbf{A}_2 - \mathbf{D}_2)^T\boldsymbol{\Pi}_2(\mathbf{A}_2 - \mathbf{D}_2)\right] \\ & + tr[\mathbf{A}_3{}^T\boldsymbol{\Pi}_3\mathbf{A}_3] + tr[\mathbf{A}_4{}^T\boldsymbol{\Pi}_4\mathbf{A}_4], \end{aligned} \tag{18}$$

where tr[M] is the trace of matrix M, P and $\boldsymbol{\Pi}_i$ for i=1,2,...,4, are positive definite matrices to be determined later.

Taking the time derivative of (18) and simplifying the resulting expression yield

$$\begin{aligned} \dot{v}(t) \;=\; & \mathbf{e}^T(\mathbf{P}\mathbf{D} + \mathbf{D}^T\mathbf{P})\mathbf{e} \\ & + 2tr\left[(\mathbf{A}_1 - \mathbf{D}_1)^T(\boldsymbol{\Omega}\mathbf{l}_e{}^T + \boldsymbol{\Pi}_1\dot{\mathbf{A}}_1)\right] \\ & + 2tr\left[(\mathbf{A}_2 - \mathbf{D}_2)^T(\boldsymbol{\Omega}\dot{\mathbf{l}}_e^T + \boldsymbol{\Pi}_2\dot{\mathbf{A}}_2)\right] \\ & - 2tr\left[\mathbf{A}_3{}^T(\boldsymbol{\Omega}\mathbf{l}_d{}^T - \boldsymbol{\Pi}_3\dot{\mathbf{A}}_3)\right] \\ & - 2tr\left[\mathbf{A}_4{}^T(\boldsymbol{\Omega}\dot{\mathbf{l}}_d^T - \boldsymbol{\Pi}_4\dot{\mathbf{A}}_4)\right] \end{aligned} \tag{19}$$

where

$$\boldsymbol{\Omega} = [\mathbf{P}_2 \;\; \mathbf{P}_3]\mathbf{z}(t) = -\mathbf{P}_2\mathbf{l}_e - \mathbf{P}_3\dot{\mathbf{l}}_e \tag{20}$$

and $\mathbf{P}$ is denoted by

$$\mathbf{P} = \begin{bmatrix} \mathbf{P}_1 & \mathbf{P}_2 \\ \mathbf{P}_2 & \mathbf{P}_3 \end{bmatrix} \tag{21}$$

and it is remarked that $\mathbf{e}(t) = -z(t)$ since $\mathbf{z}_m(t) = 0$.

We note that ξ_i and ω_i can be selected so that $\mathbf{D}$ is a *Hurwitz* matrix defined as a matrix whose eigenvalues all have negative real parts [14]. Therefore according to *Lyapunov theorem*, there exists a positive definite symmetric matrix $\mathbf{P}$ that satisfies the Lyapunov equation

$$\mathbf{PD} + \mathbf{D}^T\mathbf{P} = -\mathbf{Q}, \tag{22}$$

for any given positive-definite symmetric matrix $\mathbf{Q}$.

Now in (19), if we set

$$\boldsymbol{\Omega}\mathbf{l}_e{}^T + \boldsymbol{\Pi}_1\dot{\mathbf{A}}_1 = \boldsymbol{\Omega}\dot{\mathbf{l}}_e^T + \boldsymbol{\Pi}_2\dot{\mathbf{A}}_2 = 0 \tag{23}$$

and

$$\boldsymbol{\Omega}\mathbf{l}_d{}^T - \boldsymbol{\Pi}_3\dot{\mathbf{A}}_3 = \boldsymbol{\Omega}\dot{\mathbf{l}}_d^T - \boldsymbol{\Pi}_4\dot{\mathbf{A}}_4 = 0, \tag{24}$$

then (19) becomes

$$\dot{v}(t) = -\mathbf{e}^T\mathbf{Q}\mathbf{e} \tag{25}$$

which is a negative definite function of $\mathbf{e}(t)$. Furthermore, from (23)-(24), we otain

$$\dot{\mathbf{A}}_1 = -\boldsymbol{\Pi}_1^{-1}\boldsymbol{\Omega}\mathbf{l}_e{}^T; \;\; \dot{\mathbf{A}}_2 = -\boldsymbol{\Pi}_2^{-1}\boldsymbol{\Omega}\dot{\mathbf{l}}_e^T, \tag{26}$$

and

$$\dot{\mathbf{A}}_3 = \boldsymbol{\Pi}_3^{-1}\boldsymbol{\Omega}\mathbf{l}_d{}^T; \;\; \dot{\mathbf{A}}_4 = \boldsymbol{\Pi}_4^{-1}\boldsymbol{\Omega}\dot{\mathbf{l}}_d^T. \tag{27}$$

We already showed that $\mathbf{P}$ is a positive definite matrix. Now if we could show that $\boldsymbol{\Pi}_i$ for i=1,2,...,4, are also positive definite matrices, then the error system described in (17) is asymptotically stable, i.e., $\mathbf{e}(t) \to 0$, or $\mathbf{z}(t) \to \mathbf{z}_m$ as $t \to \infty$.

As specified in previous section, since the telerobot end-effector will perform slow and precise motion, $\mathbf{M}$, $\mathbf{N}$ and $\mathbf{G}$ are *slowly time-varying matrices* which can be considered as *nearly constant matrices.* In this case, from (8) and (9) we obtain

$$\dot{\mathbf{A}}_1 \simeq \mathbf{M}^{-1}\dot{\mathbf{K}}_p; \;\; \dot{\mathbf{A}}_2 \simeq \mathbf{M}^{-1}\dot{\mathbf{K}}_d \tag{28}$$

and

$$\dot{\mathbf{A}}_3 \simeq 0; \;\; \dot{\mathbf{A}}_4 \simeq 0. \tag{29}$$

Next substituting (28)-(29) into (26)-(27) results in

$$\mathbf{M}^{-1}\dot{\mathbf{K}}_p = -\boldsymbol{\Pi}_1^{-1}\boldsymbol{\Omega}\mathbf{l}_e{}^T; \;\; \mathbf{M}^{-1}\dot{\mathbf{K}}_d = -\boldsymbol{\Pi}_2^{-1}\boldsymbol{\Omega}\dot{\mathbf{l}}_e^T, \tag{30}$$

and

$$0 \simeq \boldsymbol{\Pi}_3^{-1}\boldsymbol{\Omega}\mathbf{l}_d{}^T; \;\; 0 \simeq \boldsymbol{\Pi}_4^{-1}\boldsymbol{\Omega}\dot{\mathbf{l}}_d^T. \tag{31}$$

Now in (30), if we let

$$\boldsymbol{\Pi}_1 = -\frac{1}{\alpha_1}\mathbf{M}; \;\; \boldsymbol{\Pi}_2 = -\frac{1}{\alpha_2}\mathbf{M}, \tag{32}$$

where α_1 and α_2 are arbitrary positive scalars, then solving for $\dot{\mathbf{K}}_p$ and $\dot{\mathbf{K}}_d$, we get

$$\dot{\mathbf{K}}_p = \alpha_1 \boldsymbol{\Omega} \mathbf{l}_e^T, \tag{33}$$

and

$$\dot{\mathbf{K}}_d = \alpha_2 \boldsymbol{\Omega} \dot{\mathbf{l}}_e^T. \tag{34}$$

We observe that in (32), $\boldsymbol{\Pi}_1$ and $\boldsymbol{\Pi}_2$ are positive definite matrices that can be considered as nearly constant because M, the end-effector mass matrix is positive definite and slowly time-varying. To satisfy (31), $\boldsymbol{\Pi}_3$ and $\boldsymbol{\Pi}_4$ should be chosen such that their determinants approach infinitive in addition to the positive definite property. Obviously $\boldsymbol{\Pi}_3$ and $\boldsymbol{\Pi}_4$could be selected such that they are diagonal matrices whose main diagonal elements are all positive and very large.

We proceed to integrate both sides of (33) and (34) to obtain

$$\mathbf{K}_p(t) = \mathbf{K}_p(0) + \alpha_1 \int_0^t (\mathbf{P}_2 \mathbf{l}_e + \mathbf{P}_3 \dot{\mathbf{l}}_e) \mathbf{l}_e^T dt \tag{35}$$

and

$$\mathbf{K}_d(t) = \mathbf{K}_d(0) + \alpha_2 \int_0^t (\mathbf{P}_2 \mathbf{l}_e + \mathbf{P}_3 \dot{\mathbf{l}}_e) \dot{\mathbf{l}}_e^T dt \tag{36}$$

where $\mathbf{K}_p(0)$ and $\mathbf{K}_d(0)$ are initial conditions of $\mathbf{K}_p(t)$ and $\mathbf{K}_d(t)$, respectively and can be set arbitrarily.

Equations (35) and (36) provide the solutions for the controller gain matrices of the adaptive controller, which are based on the lenght errors and their derivatives.

4 COMPUTER SIMULATION

In order to examine the performance of the developed joint-space adaptive control scheme, we implement it on a 2 DOF end-effector that represents a special case of the 6 DOF end-effector. As Figure 3 illustratest the structured of the 2 DOF end-effector that is mainly composed of 2 ball-screw linear actuators driven by dc motors and hung below a stationary platform via pin joints. Position feedback is accomplished by 2 linear voltage differential transformers mounted along the actuator links, Based on the diagram given in Figure 4, the cartesian position x and y expressed with respect to a reference coordinate system affixed to the stationary platform are related to the joint positions $\mathbf{l}_1$ and $\mathbf{l}_2$ as follows:

$$x = \frac{l_1^2 - l_2^2 + d^2}{2d} \tag{37}$$

and

$$y = -\frac{\sqrt{4d^2 l_1^2 - (l_1^2 - l_2^2 + d^2)^2}}{2d} \tag{38}$$

where d is the distance between the pin joints hanging the actuators. Using Lagrangian formulation, we derive the following dynamic model of the end-effector:

$$\tau(t) = \mathbf{M}(\mathbf{l},\dot{\mathbf{l}})\,\ddot{\mathbf{l}}(t) + \mathbf{N}(\mathbf{l},\dot{\mathbf{l}})\,\dot{\mathbf{l}}(t) + \mathbf{G}(\mathbf{l},\dot{\mathbf{l}}) \tag{39}$$

where

$$\tau(t) = (\tau_1 \;\; \tau_2)^T; \;\; \mathbf{l} = (l_1 \;\; l_2)^T \tag{40}$$

where τ_i and l_i denote the joint force to and the lenght of the ith actuator for i=1,2, respectively. In addition

$$\mathbf{M} = \begin{bmatrix} m_1 & 0 \\ 0 & m_1 \end{bmatrix} \tag{41}$$

$$\mathbf{N} = \begin{bmatrix} 0 & \frac{m_1 l_m (l_2 - l_1)}{3u} \\ \frac{m_1 l_m (l_1 - l_2)}{3u} & 0 \end{bmatrix} \tag{42}$$

$$\mathbf{G} = (G_1 \;\; G_2)^T \tag{43}$$

with

$$G_1 = \frac{\left\{ \begin{array}{l} -mgl_m[2l_1^2 u_1(l_1 + l_2) - l_2 u^2] \\ -m_1 g[2u_1 l_1^2(l_1 l_m + l_2 l_m + 2l_1 l_2) - l_2 l_m u^2] \end{array} \right\}}{4dl_1^2 l_2 u} \tag{44}$$

$$G_2 = \frac{\left\{ \begin{array}{l} -mgl_m[2l_2^2 u_2(l_1 + l_2) - l_1 u^2] \\ -m_1 g[2u_2 l_2^2(l_1 l_m + l_2 l_m + 2l_1 l_2) - l_2 l_m u^2] \end{array} \right\}}{4dl_1^2 l_2 u} \tag{45}$$

and

$$u_1 = l_2^2 - l_1^2 + d^2; \;\; u_2 = l_2^2 - l_1^2 + d^2; \;\; u = \sqrt{4d^2 l_1^2 - u_2}, \tag{46}$$

where m is the mass of the moving part of the link, m the total mass of the link, and l_m the fixed lenght of the actuators and g the gravitational acceleration.

In this study, we implement the developed adaptive control scheme to control the Cartesian position of the above 2 DOF end-effector tracking a desired path, which is shown in Figure 5. Three study cases are considered below where the performance of the adaptive control scheme will be compared with that of a fixed-gain control scheme developed earlier [15]. For the graphs given in Figures 6-8, solid line presents the desired path, dashed line and dashed-dotted line present the actual paths obtained from the adaptive and fixed-gain control schemes, respectively.

4.1 Tracking a Straight Line

The end-effector is controlled to track a straight line specified by $y = x + 42$ [*in cm*]. Computer simulation results as shown in Figure 6 indicates that a steady-state error of 4mm in both horizontal and vertical axes exists in the case of fixed-gain control scheme while in the case of adaptive control scheme, the steady-state error is reduced to 1 mm in horizontal axis and to 0.1 mm in vertical axis. In the case of the adaptive control scheme, it is interesting to note that at the beginning of the path, some minor deviation from the desired path occurs because the adaptive controller was trying to adapt to the end-effector dynamics.

4.2 Tracking a Sinusoidal Path

In this case we study the tracking of a sinusoidal path described by the equation $y = sin(2x - 50) - 83$ $[in\ cm]$. Simulation results presented in Figure 7 show that using fixed-gain control scheme, the robot tracks the desired path with a maximum deviation of 1.5 mm and 3 mm in horizontal and vertical directions, respectively, while with adaptive control scheme, the tracking quality is improved in the sense that the maximum deviation along the horizontal and vertical axes are reduced to 0.8 mm and 0.1 mm, respectively. Unlike the straight line case, faster adaptation occurs in the current study case as showed in the beginning of the path.

Tracking a Circular Path

Figure 8 presents the simulation results of tracking a circular path defined by the equaiton $(x - 34)^2 + (y + 83)^2 = 16$ $[in\ cm]$. Comparative evaluation of the results of the two applied control schemes shows that the steady-state errror is much smaller in the case of adaptive control scheme compared to the case of fixed-gain control scheme. In particular, the fixed gain and adaptive control schemes have a steady-state error of 3mm and 0.1mm, respectively in both horizontal and vertical axes.

In the above simulation study, the control scheme parameters were set as follows:

- *Fixed-Gain Control Scheme*: $K_{p_1} = K_{p_2} = 3000N/m$ and $K_{d1} = K_{d2} = 90N.sec/m$.
- *Adaptive Control Scheme*: ξ_i and ω_i for i=1,2 were selected so that 2 characteristic roots are both located at -10. Thus $\mathbf{D}_1=100\mathbf{I}_2$ and $\mathbf{D}_2=20\mathbf{I}_2$.

5 CONCLUSION

A joint-space adaptive control scheme was developed in this report to control the motion of a 6 DOF end-effector mounted to the slave arm of a telerobotic system to perform assembly tasks in the traded mode of a teleoperation. The adaptive control scheme consists of a proportional and a derivative time varying controllers designed by employing the concept of model reference adaptive control and Lyapunov theorem. The joint-space adaptation scheme was derived under the assumption that the end-effector performs slow motion so that the end-effector mass matrix can be considered as *nearly constant*. Unlike other nonlinear control schemes for robot manipulators, the developed control scheme does not require the computation of the end-effector dynamics. Therefore this computationally efficient control scheme can be implemented in real-time control applications without the requirement of a super fast computer. Implementation of the developed control scheme on a 2 DOF end-effector was investigated using computer simulation. We considered three different cases of path tracking: tracking a straight line, tracking a sinusoidal path, and tracking a circular path and compared the performance of the adaptive control scheme with a fixed-gain controller scheme. Simulation results showed that the adaptive control scheme provides better tracking performance with smaller steady-state errors than the fixed-gain control scheme. Future research should be focused on the development of Cartesian-space adaptive control schemes and hybrid adaptive control schemes [15] and extend the developed adaptive control scheme to handle fast robot motion.

References

[1] JPL, "Telerobotics Project Plan," *Jet Propulsion Laboratory*, JPL D-5692, August 1988.

[2] Nguyen, C.C., Pooran F.J., "Kinematic Analysis and Workspace Determination of a 6 DOF CKCM Robot End-Effector," *Journal of Mechanical Working Technology*, Vol. 20, pp. 283-294, June 1989.

[3] Arimoto, S., Miyazaki, F., "Stability and Robustness of PID Feedback Control for Robot Manipulators of Sensory Capability," *Third International Symposium of Robotics Research*, Gouvieux, France, July 1985.

[4] Hsia, T.C., "Adaptive Control of Robot Manipulators: A Review," *Proc. IEEE Conf. on Robotics and Automation*, San Francisco, pp. 183-189, 1986.

[5] Craig, J.J., *Adaptive Control of Mechanical Manipulators*, Addison-Wesley, Reading, Massachusetts, 1988.

[6] Seraji, H., "A New Approach to Adaptive Control of Manipulators,", *ASME Journal of Dynamic Systems, Measurement, and Control*, Vol. 109, pp. 193-202, 1987.

[7] Lim, K.Y., and Eslami, M., "Robust Adaptive Controller Designs For Robot Manipulator Systems," *Proc. IEEE Conf. on Robotics and Automation*, San Francisco, pp. 1209-1215, 1986.

[8] Daneshmend, L.K. and Pak, H.A., "Model Reference Adaptive Control of Feed Force in Turning," *Trans. ASME, Journal of Dynamic Systems, Measurement, and Control*, Vol. 108, pp. 215-222, September, 1986.

[9] Houshangi, N. and Koivo, A.J., "Eigenvalue Assignment and Performance Index Based Force-Position Control with Self-Tuning For Robotic Manipulators," *Proc. IEEE Conf. on Robotics and Automation*, pp. 1386-1391, 1987.

[10] Seraji, H., "Adaptive Force and Position Control of Manipulators," *Journal of Robotics Systems*, 4(4), pp. 551-578, 1987.

[11] Nguyen, C.C., Pooran, F.J., "Adaptive Force/Position Control of Robot Manipulators with Closed-Kinematic Chain Mechanism," in *Robotics and Manufacturing: Recent Trends in Research, Education, and Application*, Chapter 4, edited by M. Jamshidi et al, ASME Press, New York, pp. 177-186, 1988.

[12] Premack, Timothy et al, "Design and Implementation of a Compliant Robot with Force Feedback and Strategy Planning Software," *NASA Technical Memorandum 86111*, 1984.

[13] Stewart, D., "A Platform with Six Degrees of Freedom," *Proc. Institute of Mechanical Engineering*, vol. 180, part 1, No. 5, pp. 371-386, 1965-1966.

[14] Landau, Y.D., *Adaptive Control: The Model Reference Approach*, Marcell Dekker, New York, 1979.

[15] Nguyen, C.C., Pooran, F.J. and Premack, T., "Trajectory Control of Robot Manipulator with Closed-Kinematic Chain Mechanism," *Proc. 20th Southeastern Symposium on System Theory*, North Carolina, pp. 454-458, March 1988.

[16] Nguyen, C.C., Pooran F.J., "Joint-Space Adaptive Control of Robot End-Effectors Performing Slow and Precise Motions," *Proc. 21th Southeastern Symposium on System Theory*, Florida, pp. 547-552, March 1989.

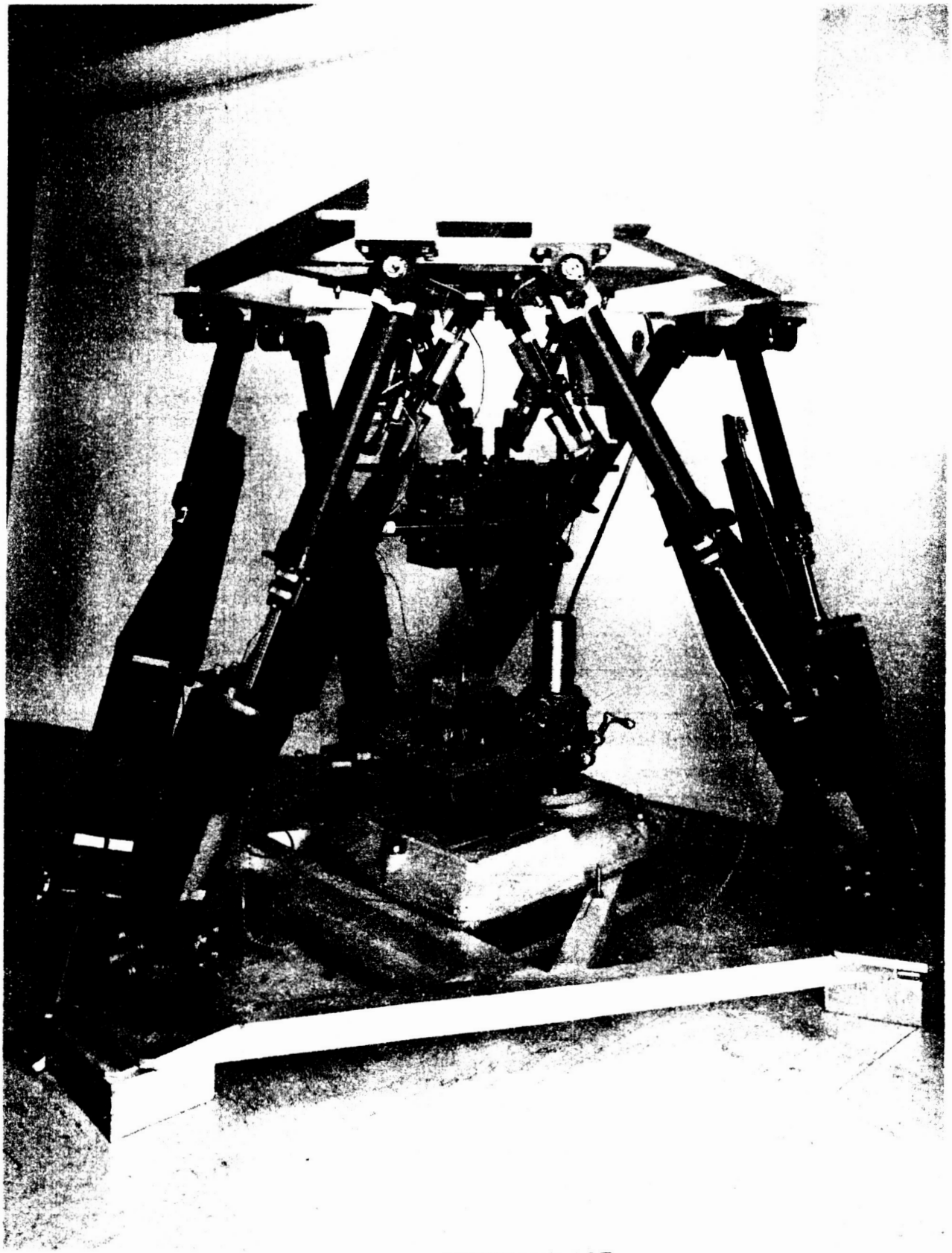

ORIGINAL PAGE
BLACK AND WHITE PHOTOGRAPH

Figure 1: The NASA Robot End-Effector

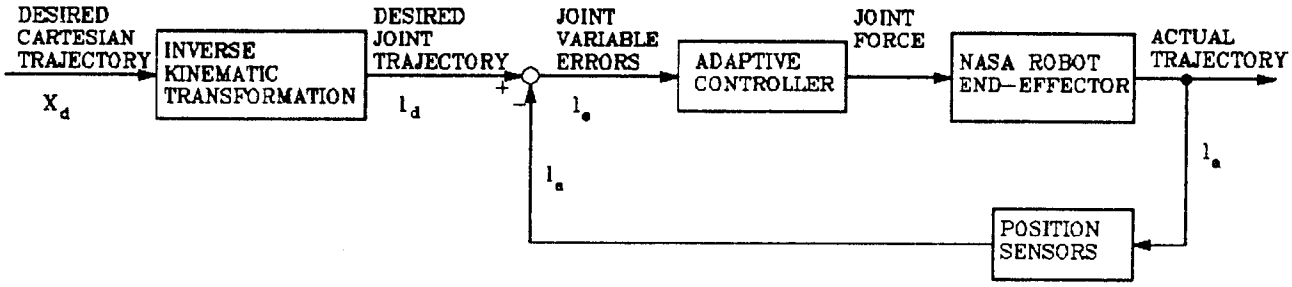

Figure 2: The joint-space adaptive control scheme

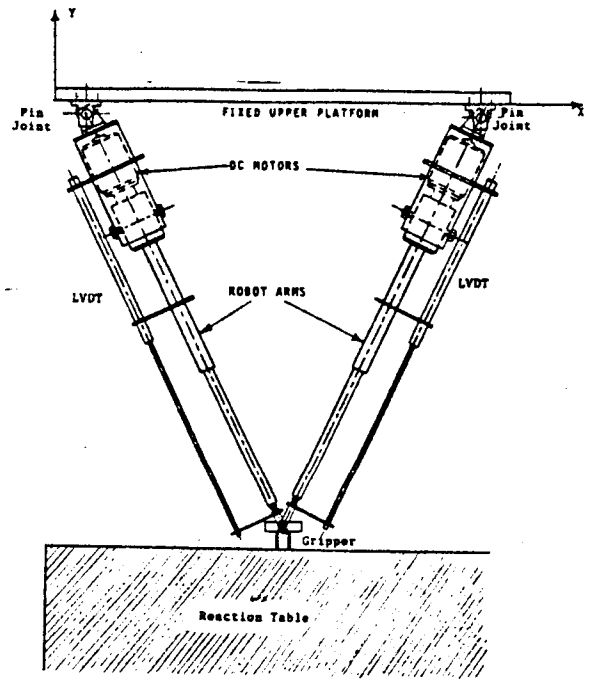

Figure 3: The 2 DOF end-effector

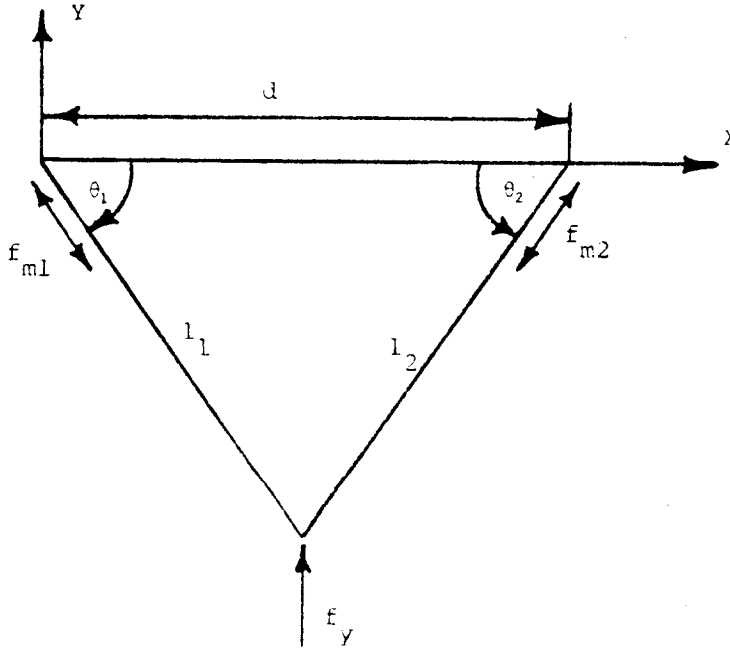

Figure 4: Free body diagram

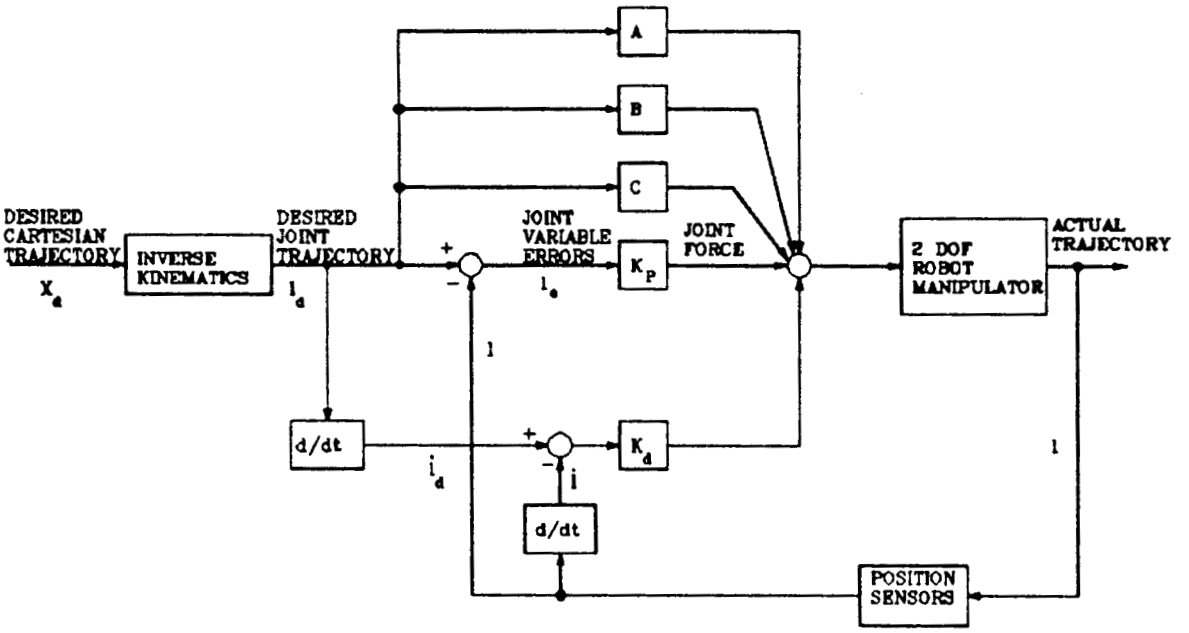

Figure 5: Implementation of the joint-space adaptive control scheme

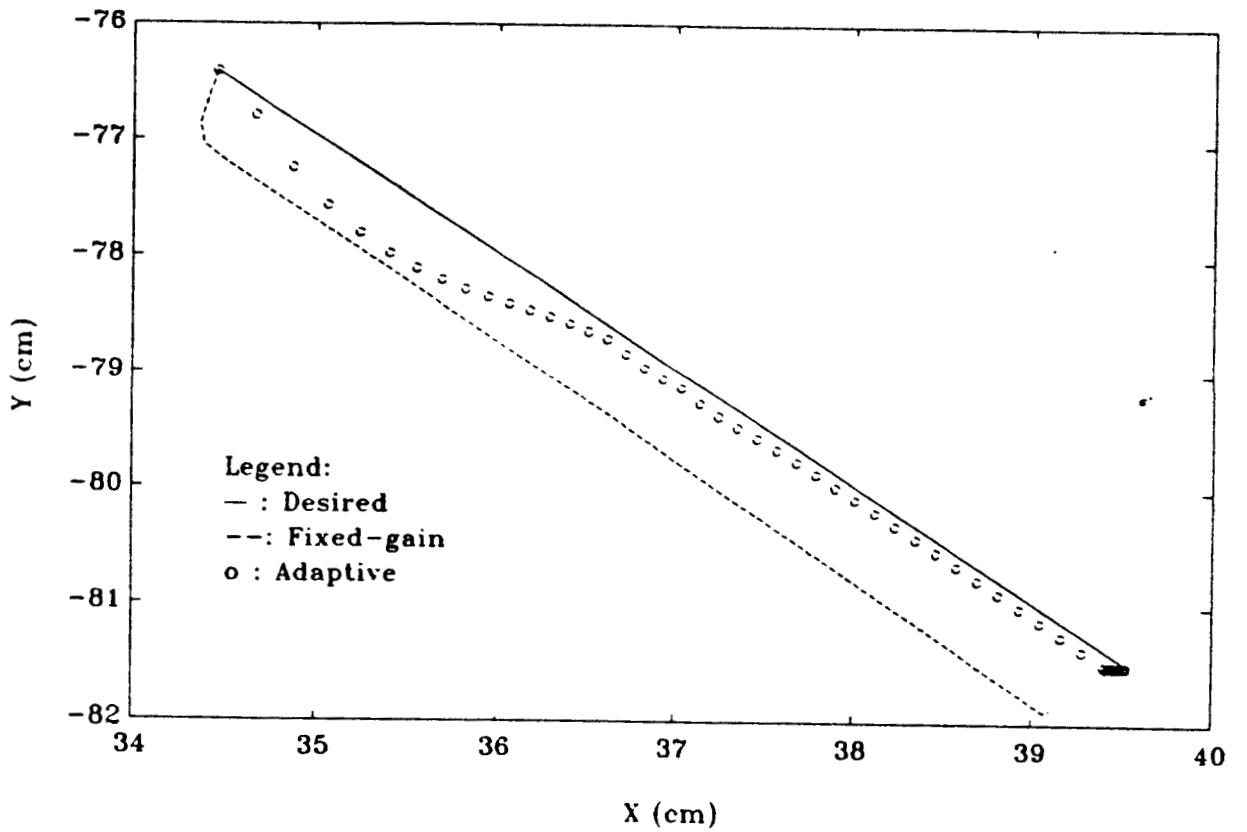

Figure 6: Computer simulation result for tracking a linear path

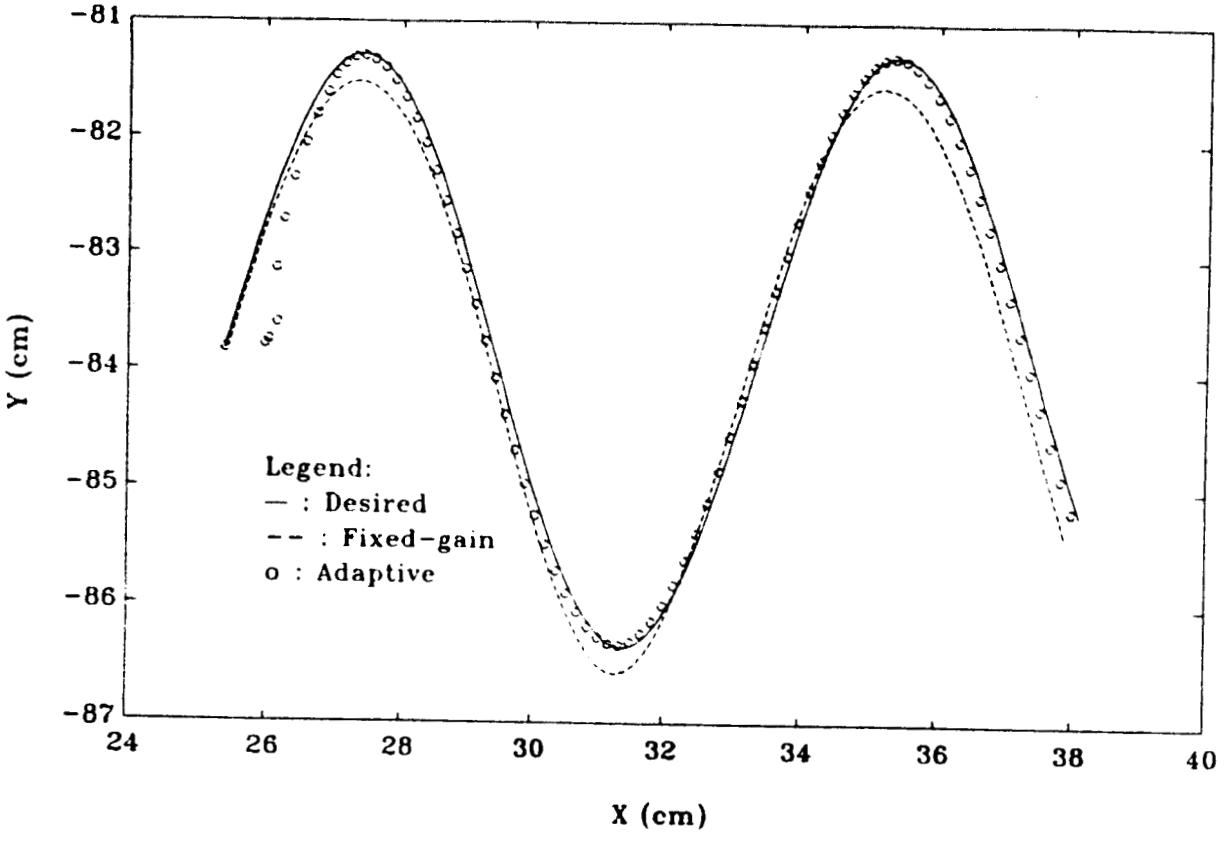

Figure 7: Computer simulation result for tracking a sinusoidal path

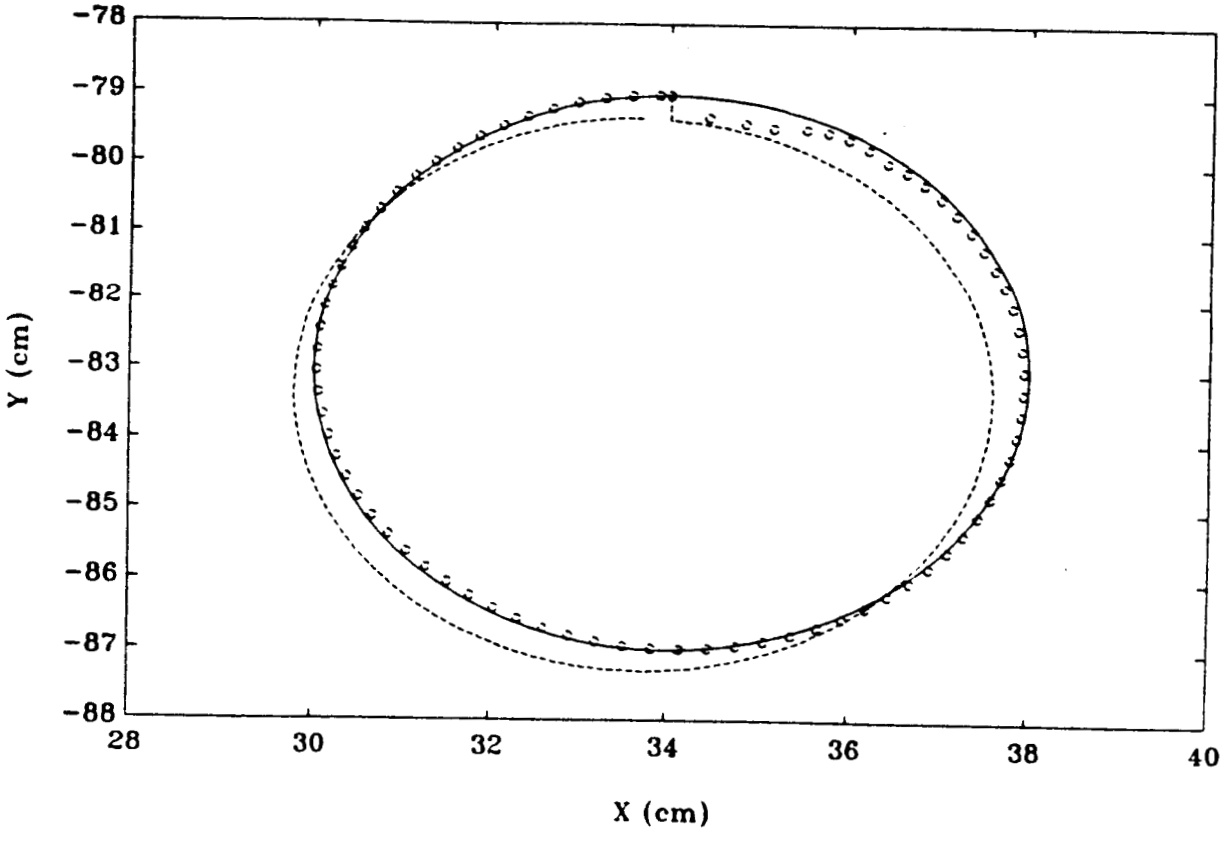

Figure 8: Computer simulation result for tracking a circular path